WEP Warwick Evans Publishing

International Journal of Natural Resources and Environmental Studies

ISSN: 3006-2012 (Print), ISSN: 3006-0834 (Online) | Volume 2, Number 1, Year 2024
DOI: https://doi.org/10.62051/ijnres.v2n1.29
Journal homepage: https://wepub.org/index.php/IJNRES/index

Attribution Analysis of Discharge Variations in the Inner Mongolia Basin of the Yellow River

Yongxiao Guo[1, *]

[1]School of Surveying and Land Information Engineering, Henan Polytechnic University, Jiaozuo 454000, China

*Corresponding Author: Yongxiao Guo (E-mail: 212104020076@home.hpu.edu.cn)

ABSTRACT

Climate change and human activities are the main causes of discharge variation. Therefore, calculating the contribution of climate change and human activities to discharge variation in the Inner Mongolia Basin of the Yellow River can provide a reference basis for alleviating water resources stress in the Inner Mongolia Basin of the Yellow River. Firstly, based on the water balance theory and the Budyko hypothesis-based evapotranspiration formula, this study constructed a coupled water and heat balance equation and calibrated and validated the model using observed annual discharge depth data from the Toudao Guai hydrological station. The results show that the water-heat coupling model has good simulation accuracy at the annual scale, with NSE=0.76, RMSE=10.45, and RRMSE=19.5%, and overall, the simulated discharge results are close to the observed values. Secondly, this study also used the Mann-Kendall test method to determine the abrupt change points of discharge and analyzed the contribution rates of various meteorological factors. The results indicate that precipitation accounts for 88.79% of the discharge variation in the Inner Mongolia segment of the Yellow River basin, followed by land surface changes at 13.6%, while potential evaporation has the smallest contribution to discharge variation.

KEYWORDS

Discharge variation, attribution analysis, Inner Mongolia section of the Yellow River, climate change.

1. INTRODUCTION

Land water is a critical indicator of inland hydrological conditions, highly sensitive to changes in land use and land cover, natural disasters, and climate variations. Its quantity, quality, and spatiotemporal distribution characteristics have significant impacts on ecological balance, human security, and economic development(Jia et al., 2018,Song et al.,2019). In recent years, global climate anomalies and issues such as water scarcity and uneven spatial and temporal distribution of water resources have become increasingly apparent. Consequently, there has been a growing body of research on surface water resource monitoring, which is a vital component of water resources, both domestically and internationally(Song et al.,2005.,Zhang et al., 2011,Klemes et al., 2020).

Climate change and land surface modifications can induce variations in basin discharge. The integration of remote sensing data with hydrological models offers possibilities for estimating basin discharge. Currently, the quantification of the impact of climate-induced land surface changes on discharge involves parameters such as precipitation, potential evapotranspiration, land use characteristics, and vegetation cover elements. Combining these factors with the Budyko hypothesis and water balance equations enables an effective analysis of basin discharge variations. Ning et al.(2017) discussed the relationship between parameters, vegetation coverage, and climate change

based on the framework of the Budyko theory, indicating a strong correlation among these factors. Gan et al.(2021) investigated the hydrological effects of vegetation dynamics under climate change based on the Budyko model. The results indicated that although climate governs watershed water balance, vegetation often plays a more significant role than climate change. Additionally, the impact of vegetation on annual discharge is most pronounced in regions with limited water resources. Gichamo et al.(2023) conducted a study on ensemble rainfall-discharge modeling in the Blue Nile Basin of Ethiopia using the Hydraulic Modeling System and Hydrologiska Byråns Vattenbalansavdelning,the results indicate a significant improvement in rainfall-discharge modeling with the rainfall fusion model compared to satellite rainfall modeling (efficiency improved by 13.3%). This underscores the importance of integrating multisource rainfall datasets for rainfall-discharge simulation in ungauged basins.

Currently, there is a growing interest in exploring the attribution of discharge changes to meteorological data, aiming to better understand variations in watershed water resources. Shi et al.(2020) analyzed the variation patterns of Budyko parameters based on the hydro-thermal coupling Budyko equation, using different climatic characteristics of the Songhua River Basin, Yellow River Source Area, and Pearl River Basin， they combined this analysis with predictions of future water resources for the three basins under three scenarios from four climate models in CMIP5. Zhang et al.(2022) established a hydro-thermal coupling model suitable for the Zhenjiangguan Basin based on the Fu Baopu formula under the Budyko hypothesis. By quantifying the impact of climate change and land surface changes on discharge in the Zhenjiangguan Basin through parameterization of land surface characteristics, the results indicate that climate change remains the dominant factor influencing discharge variation. Yan et al.(2023) analyzed the effects of evapotranspiration, precipitation, and land surface changes on discharge variation in the Jinxi Basin using meteorological and hydrological data, and the Budyko hydro-thermal coupling balance equation theory.

Overall, the water balance equation based on the Budyko hydro-thermal coupling balance theory has achieved significant results in attributing discharge changes in the study area. Therefore, this study will utilize the hydro-thermal coupling balance equation to conduct an attribution analysis of discharge changes in the Inner Mongolia section of the Yellow River, which will contribute to understanding the hydrological process variations in the region and facilitate precise management of regional water resources.

2. RESEARCH AREA AND DATA

2.1. Research Area

The Inner Mongolia section of the Yellow River Basin is located in the upstream part of the Yellow River Basin, between 106°58'E-111°10'E and 40°15'N-40°50'N. It has a "J"-shaped distribution with a drainage area of $1.51\times10^4 m^3$. The Inner Mongolia section of the Yellow River starts from the entry point at Lapsang Temple in Ordos, Inner Mongolia, passing through Shizuishan City in Ningxia, and exits at Yushuwan in Magai County, Zunge'er Banner, Ordos City. Along the way, the Yellow River flows through various regions of Inner Mongolia Autonomous Region, including Ulanqab, Bayannur, Baotou, and Hohhot. The main stream has a length of 842km, with a total drop of only 162.5m (Yang, 2021). The Inner Mongolia section of the Yellow River possesses diverse natural resources such as grasslands, lakes, wetlands, and deserts. Therefore, a precise understanding of its discharge variation can effectively facilitate water resource management and maximize resource utilization.

2.2. GLDAS-Noah Data

The Global Land Data Assimilation System (GLDAS) is a joint development project between NASA of the United States and JAXA of Japan. Its main purpose is to utilize advanced land surface modeling and data assimilation techniques to extract satellite and ground-based data and integrate them into

optimal models. (Rodell and Houser et al. 2004)。Currently, the GLDAS system consists of four land surface models (LSMs), namely Mosaic, CLM2, Noah, and VIC. In this study, the rainfall data primarily utilized the land surface model of the Noah model.

2.3. GLEAM Data

This study also utilized potential evapotranspiration data derived from GLEAM (Global Land Evaporation Amsterdam Model). GLEAM is an algorithm that estimates global-scale evapotranspiration by combining satellite observations and utilizing the Priestley and Taylor equation (Miralles and Holmes et al. 2011). Since 2011, GLEAM has been continuously revised and updated, with the third version of the model being released by 2017.

2.4. Observation Data

The discharge depth refers to the depth of water spread over the watershed area upstream of a station, reflecting the water resource conditions of the controlled watershed at the station. The observed discharge depth data used in this study are from the Taodao River Hydrological Station, documented in the Yellow River Hydrological Statistical Yearbook, covering the period from 2003 to 2020. These data are utilized for parameter calibration and accuracy validation of the model. As an important monitoring station in the Inner Mongolia section of the Yellow River Basin, the Taodao River Hydrological Station's long-term accumulated discharge data holds significant importance for studying hydrological changes in the Yellow River Basin.

3. METHODS

3.1. Hydrothermal Coupling Balance Theory

Based on the Budyko hydrothermal coupling balance hypothesis, the hydrothermal coupling balance equation for the watershed is derived, and the impact of climate change and human activities on discharge is analyzed. According to the principle of water balance, under certain climatic and vegetation conditions, the hydroclimatic characteristics of the watershed conform to the following water and energy balance relationship:

$$R = P - E + \Delta S \tag{1}$$

Where R is the discharge depth,mm; P is precipitation,mm; E is actual evapotranspiration,mm; ΔS is the change in watershed water storage,mm, which is close to zero on an annual or multi-year scale. The changes in precipitation, evapotranspiration, and water storage can be obtained through remote sensing methods.

Yang et al.(2008) derived the watershed hydrothermal coupling balance equation based on the Budyko hydrothermal coupling balance assumption, indicating that under certain climate and vegetation conditions, the hydroclimate characteristics of the watershed conform to the water and energy balance relationship as follows:

$$E = \frac{P \times ET_0}{(P^n + ET_0^n)^{\frac{1}{n}}} \tag{2}$$

Where E is the actual annual evapotranspiration; ET_0 is the annual potential evapotranspiration; P is the annual precipitation; n is the land surface parameter (dimensionless), which is related to soil properties, terrain, and vegetation.

Combining equations (1) and (2), and at an annual scale, which can be neglected, the model can be expressed as follows:

$$R = P - \frac{P \times ET_0}{(P^n + ET_0^n)^{\frac{1}{n}}} \tag{3}$$

3.2. 3.2 Analysis Method of Discharge Variation

The elasticity coefficient is the ratio of the rate of change of the dependent variable to the rate of change of the independent variable. The discharge elasticity coefficient refers to the ratio of the rate of change of discharge to the rate of change of the driving factor:

$$\varepsilon = \frac{\mathrm{d}R / R}{dX / X} \tag{4}$$

Where R is the discharge depth; X is a driving factor, such as precipitation, evapotranspiration, and land surface changes.

The changes in discharge caused by different climatic factors can be estimated by the product of variations in each climatic factor and their partial derivatives. Therefore, the multi-year average discharge depth change can be represented as follows in total differential form(Yang et al., 2023):

$$\frac{\mathrm{d}R}{R} = \varepsilon P \frac{\mathrm{d}P}{P} + \varepsilon E_0 \frac{\mathrm{d}E_0}{E_0} + \varepsilon \mathrm{n} \frac{\mathrm{dn}}{\mathrm{n}} \tag{5}$$

Utilizing equation (5) and combining it with the definition of elasticity coefficient, we can derive the precipitation elasticity coefficient, potential evapotranspiration elasticity coefficient, and land surface elasticity coefficient. The calculation formulas are as follows: (Ning and Tingting et al. 2016):

$$\varepsilon_p = \frac{(1+\phi^n)^{\frac{1}{n}+1} - \phi^{\mathrm{n}+1}}{(1+\phi^n)\left[(1+\phi^n)^{\frac{1}{\mathrm{n}}} - \phi\right]} \tag{6}$$

$$\varepsilon_{E_0} = \frac{1}{(1+\phi^n)\left[1-(1+\phi^{-n})^{\frac{1}{\mathrm{n}}}\right]} \tag{7}$$

$$\varepsilon_{\mathrm{n}} = \frac{\ln(1+\phi^n) + \ln(1+\phi^{-n})}{\mathrm{n}\left[(1+\phi^n) - (1+\phi^n)^{\frac{1}{\mathrm{n}}+1}\right]} \tag{8}$$

Where $\varepsilon_p, \varepsilon_{E_0}, \varepsilon_{\mathrm{n}}$ is the elasticity coefficients of precipitation, potential evapotranspiration and land surface parameters, Given that $\phi = \frac{E_0}{P}$ is obtained， which represents the aridity index.

Based on the discharge change inflection point, the study period is divided into two sub-periods: a baseline period and a changing period. Discharge is influenced by both climatic changes and changes in watershed underlying surfaces, and can be expressed as:

$$\Delta R = \Delta R_P + \Delta R_{E_0} + \Delta R_{\mathrm{n}} \tag{9}$$

Where ΔR is the difference between the baseline period and the changing period; ΔR_P、ΔR_{E_0}、ΔR_{n} is the discharge change caused by variations in precipitation, potential evapotranspiration, and land surface changes. The calculation formula is as follows(Yang and Zhang et al.2015):

$$\Delta R_P = \varepsilon_P \frac{R}{P} \Delta P \tag{10}$$

$$\Delta R_{E_0} = \varepsilon_{E_0} \frac{R}{E_0} \Delta E_0 \tag{11}$$

$$\Delta R_{\mathrm{n}} = \varepsilon_{\mathrm{n}} \frac{R}{\mathrm{n}} \Delta \mathrm{n} \tag{12}$$

Finally, the contribution rates of precipitation, potential evapotranspiration, and land surface changes to discharge variations are expressed as follows:

$$C_{x_i} = \frac{\Delta R_{x_i}}{\Delta R_P + \Delta R_{E_0} + \Delta R_n} \times 100\% \tag{13}$$

Where C_{x_i} is the contribution rates of factors P、E_0 and n to discharge variations in the watershed.

3.3. Mann-Kendall"s test

Mann-Kendall’s test does not require samples to follow a certain distribution, and the lack of some data will not affect the results. The non-parametric Mann-Kendall test was employed to detect trends and breakpoints in potential evapotranspiration, precipitation, and river discharge depth in the Inner Mongolia section of the Yellow River. Hypothesis testing based on the Mann-Kendall statistic was applied to all variables at a significance level of ∂(Zhang et al.2007).

The time series of variables $X = (x_1, x_2, x_3 \cdots\cdots x_n)$,the test statistic is calculated by the following formula：

$$S = \sum_{i=1}^{n-1} \sum_{j=i+1}^{n} \mathrm{sgn}(X_j - X_i) \tag{14}$$

Where n is the length of the time series; i , j denote the data at the i-th and j-th positions in the time series, respectively; sgn() denotes the sign function, which is calculated as follows:

$$\mathrm{sgn}(\theta) = \begin{cases} 1 & \theta > 0 \\ 0 & \theta = 0 \\ -1 & \theta < 0 \end{cases} \tag{15}$$

Mann and Kendall found that when the length of the time series is sufficiently long, usually a sequence length ≥ 8 is required, The test statistic (S) follows $N\left(\mu, \delta^2\right)$, $\mu = 0$, Variance δ^2 can be estimated as follows:

$$\delta^2 = Var(S) = \frac{n(n-1)(2n+5) - \sum_{i=1}^{n_i} t_i(i-1)(2i+5)}{18} \tag{16}$$

Where n_i is the number of groups of identical data points in the time series; t_i is the number of repetitions of identical data points within each group of identical data points; In hydrological time series, $n_i = 0$, $t_i = 0$, Therefore, the above equation can generally be simplified as follows:

$$\delta^2 = Var(S) = \frac{n(n-1)(2n+5)}{18} \tag{17}$$

Standardizing the statistic S, the formula for standardized statistics can be obtained as follows:

$$Z_c = \begin{cases} \dfrac{S-1}{\sqrt{Var(S)}} & S > 0 \\ 0 & S = 0 \\ \dfrac{S+1}{\sqrt{Var(S)}} & S < 0 \end{cases} \tag{18}$$

For a given significance level ∂ (typically set at 0.05），if$|Z| \geq Z_{1-\frac{\partial}{2}}$, the null hypothesis is rejected, indicating a significant trend in the series at the confidence level of ∂, otherwise, the null hypothesis holds, suggesting the series is not significant， if $Z > 0$, it indicates an upward trend; conversely, a downward trend exists.

3.4. Evaluation of river discharge accuracy

This paper uses the Nash-Sutcliffe efficiency coefficient (NSE), the Root Mean Squared Error (RMSE), and the Relative Root Mean Squared Error (RRMSE), with their respective calculation formulas as follows:

$$NSE = 1 - \frac{(Q_m - Q_e)^2}{(Q_m - \overline{Q_m})^2} \tag{0.1}$$

$$RMSE = \sqrt{\frac{\sum (Q_m - Q_e)^2}{n}} \tag{0.2}$$

$$RRMSE = \frac{RMSE}{\overline{Q}_m} \times 100\% \tag{0.3}$$

Where Q_m is the estimated discharge depth, Q_e is the in situ discharge depth, $\overline{Q}_m$ denotes the mean value of the in situ discharge depth, n represents the total number of observations, The *NSE* varies from $-\infty$ to 1, and 1 indicates the optimal status in which the simulated discharge equals the in situ measurements.

4. RESULTS

4.1. Calibration of model parameters

For parameter n, the observed discharge from the Head First Bend hydrological station is selected as the measured data for calibration. In this study, a genetic algorithm is employed to establish the objective function, which integrates the genetic algorithm with the coupled water and heat model to fit the data. Through several iterations, the optimal parameters are searched for, achieving the calibration and optimization of parameter n, thus realizing the discharge simulation based on the coupled water and heat model.

Genetic Algorithm (GA) is an optimization algorithm based on the biological evolution process. It simulates the process of biological evolution by mimicking natural selection, crossover, and mutation to search for optimal or near-optimal solutions. In genetic algorithms, each candidate solution to a problem is represented as a chromosome or genome. Typically, a chromosome consists of a sequence of genes, where each gene represents a part or parameter of the solution. The initial set of candidate solutions is referred to as the population. Each candidate solution in the population has an associated fitness evaluation, which measures its quality in the solution space. The main steps in implementing a genetic algorithm include the following:

(1) Initialize Population: Randomly generate a set of candidate solutions as the initial population, adhering to the format of chromosome encoding. In this study, each chromosome is represented as a real-valued vector.

(2) Evaluate Fitness: Compute the fitness evaluation of each candidate solution based on specific criteria for the problem.

(3) Selection: Based on the fitness evaluation, select some excellent individuals as parents for reproducing the next generation. Common selection methods include roulette wheel selection and tournament selection.

(4) Crossover: Generate new candidate solutions by performing crossover operations on the selected parents. This typically involves exchanging genetic segments between two or more parents.

(5) Mutation: Introduce random genetic mutations to the newly generated candidate solutions to increase the diversity of the population.

(6) Repeat Evolution: Iterate through the above steps to produce new candidate solutions until a stopping criterion is met (e.g., reaching the maximum number of iterations or finding a satisfactory solution).

(7) Select the Best Solution: Choose the candidate solution with the highest fitness from the final population as the ultimate optimization result.

This study starts from both monthly and annual scales, using measured discharge data to calibrate model parameters, and analyzes the applicability of the hydrothermal coupling model in the Inner Mongolia segment of the Yellow River Basin at different time scales. After fitting with the genetic algorithm (GA), at the annual scale, the optimal solution n = 4.452.

4.2. Evaluation of Simulation

At the annual scale, complete time series of precipitation and potential evapotranspiration(2003-2020) were selected as model inputs, with concurrent observed discharge serving as the ground truth for parameter calibration of the coupled hydrothermal model. Through GA algorithm fitting, at the annual scale, n=4.45. yielded the best model simulation performance. Figure1 shows the discharge simulation results, where the observed annual average discharge was 53.68mm, the simulated annual

discharge depth averaged 52.03mm, the annual average precipitation was 318.84mm, and the annual average potential evapotranspiration was 306.99mm.

A univariate linear regression analysis was conducted on simulated discharge and measured discharge at the TouDaoGuai Water Station, resulting in a coefficient of determination R2=0.77. The scatter plot depicting their correlation is shown in Figure 2. Overall, the simulated values are close to the observed values, indicating good accuracy of the water-heat coupling model at the annual scale and its suitability for reflecting the annual and seasonal variations in discharge depth within the watershed.

The simulation results of the water-heat coupling model in the Inner Mongolia region of the Yellow River Basin were evaluated using the Nash-Sutcliffe efficiency coefficient(NSE), the root mean squared error(RMSE), and the relative root mean squared error(RRMSE) as evaluation indicators. The calculated Nash-Sutcliffe efficiency coefficient NSE=0.76 indicates a good consistency between simulated and observed discharge. The RMSE=10.45mm and the relative root mean squared error RRMSE=19.5%, indicating satisfactory simulation performance of the water-heat coupling model at the annual scale. Specifically, for the years 2004, 2013, 2014, 2015, and 2020, the simulated discharge closely matched the observed discharge, with errors within 3mm. However, for some individual years, the predicted values generally underestimate the observed values. Overall, the simulated discharge is relatively close to the observed discharge, but there are significant discrepancies in certain years, such as 2012 and 2019, where the simulated values deviate by 17.21mm and 23.20mm lower than the observed values, respectively. This is mainly due to large differences in precipitation and evapotranspiration.

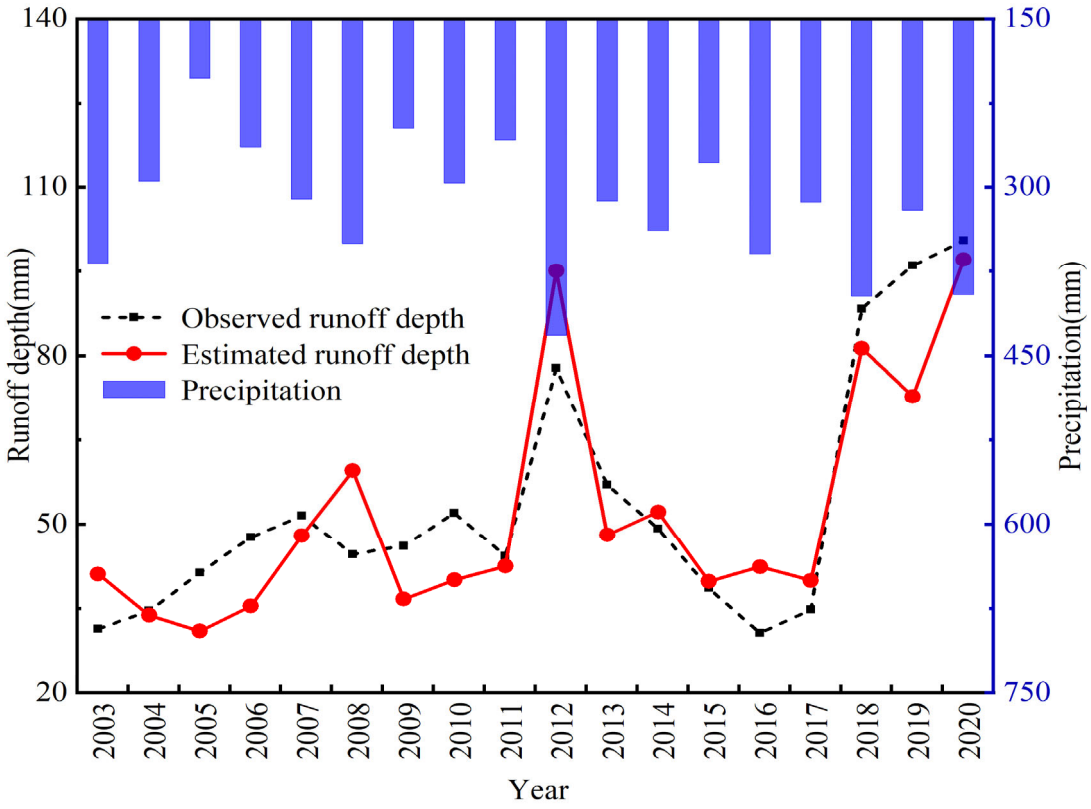

Figure 1. Comparison of simulated and observed discharge at the annual scale.

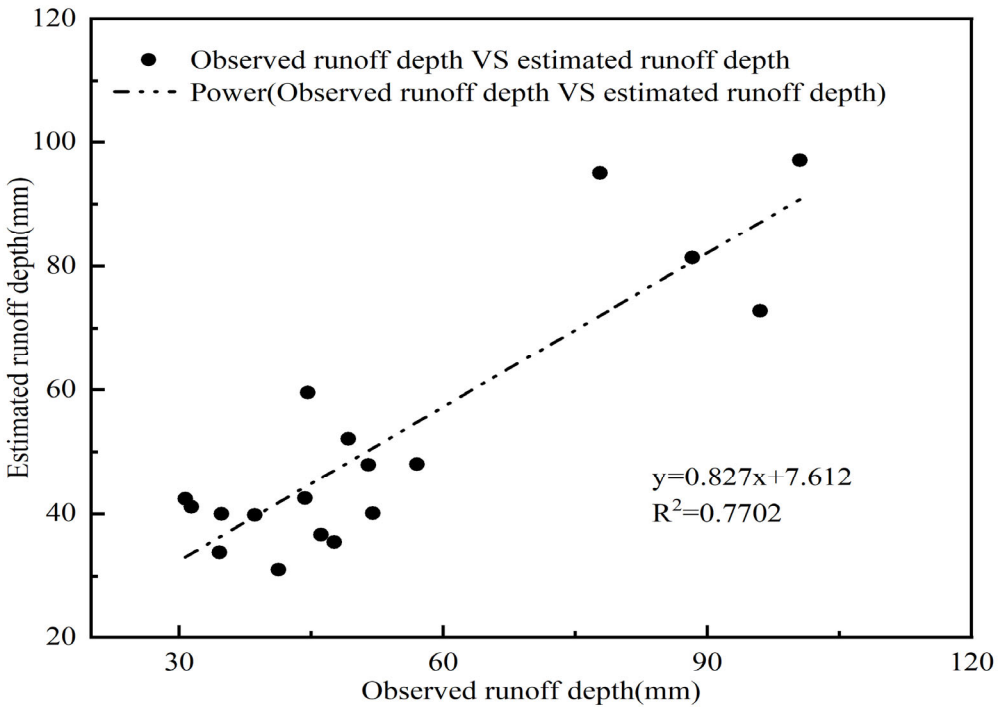

Figure 2. Scatter plot of simulated and observed discharge at the annual scale.

4.3. Sensitivity analysis of discharge

In this study, the Mann-Kendall test was applied to analyze the trends of annual potential evapotranspiration, annual discharge depth, and annual precipitation in the Inner Mongolia region of the Yellow River basin from 2003 to 2020. The results, including the detected change points within a 95% confidence interval, are summarized in Table 1. It can be observed from the table that all three meteorological elements exhibit increasing trends (statistical values falling within the intervals ((0, 1.65], (1.65, 1.96], [1.96, ∞), indicating non-significant, slightly significant, and highly significant, respectively). Among them, the annual discharge depth shows a highly significant increasing trend, while the increasing trend of annual precipitation is much greater than that of annual potential evapotranspiration. Based on the detected change points for annual discharge depth, considering the relatively short time series for the years from 2015 to 2020, the final change point for discharge depth in this region from 2003 to 2020 is determined to be the year 2012. According to the analysis of the discharge depth change point, the period from 2003 to 2012 is designated as the baseline period, during which the discharge change is considered to be less affected by climate variability and human activities. The period from 2012 to 2020 is regarded as the change period.

Table 1. The Mann-Kendall trend test results for various meteorological factors

Hydro-meteorological	Potential evapotranspiration	Precipitation	Discharge depth
Test statistic	0.68	1.89	2.12
Trend	non-significant	slightly significant	Highly significant
Turning point	2008 、2012、2015	2008、2015	2012 、2015

Table 2 presents the values of various hydrological elements and their elasticity coefficients in the Inner Mongolia region of the Yellow River Basin. Regarding meteorological hydrological elements, the multi-year average precipitation, multi-year average discharge, and multi-year average potential evaporation during the change period have increased compared to the baseline period, by 12.3%, 7.6%, and 31.3%, respectively. In terms of elasticity coefficients, during the change period, ε_P has the highest value, followed by ε_{E_0}, and lastly ε_{n}. This indicates that discharge is most sensitive to changes in precipitation, and only the value of ε_P is greater than 0，being 3.64，indicating that for every 10% increase in precipitation, discharge will increase by 36.4%. The values of ε_{E_0} and ε_{n} are -0.12 and -1.26 respectively, indicating that for every 10% increase in potential evaporation and land surface index, discharge will decrease by 1.2% and 1.26%, respectively. Compared to the reference period, the absolute values of ε_{E_0} and ε_{n} increase during the change period, indicating that land surface and potential evaporation have a greater impact on discharge changes during this period, while the absolute value of ε_P decreases compared to the reference period, indicating that the effect of precipitation on discharge changes diminishes during the change period.

Table 2. Characteristics of hydrological elements and elasticity coefficients.

period	P/mm	E_0/mm	R/mm	n	E0/P	R/P	ε_P	ε_{E_0}	ε_{n}
Complete period	318.84	306.99	53.68	4.45	0.96	0.17	3.81	-0.11	-1.14
Baseline period	302.36	296.93	47.12	4.58	0.98	0.16	3.98	-0.09	-1.03
Change period	339.43	319.56	61.89	4.31	0.94	0.18	3.64	-0.12	-1.26
Rate of change%	12.3	7.6	31.3	-5.9	4.08	12.5	-8.5	31.9	22.3

4.4. Quantitative contributions of the elements on discharge change

The contributions of P, E_0 and n to discharge changes in the Inner Mongolia section of the Yellow River Basin are shown in Table 3. The actual change in discharge ΔR_s is close to the discharge change calculated by the hydrothermal coupling model ΔR_m, indicating that the contributions obtained in this study can effectively assess the impacts of climate change (including precipitation and potential evaporation changes) and human activities on discharge due to changes in surface underlying conditions. The decrease in precipitation contributes 24.01mm to discharge changes, with a high contribution rate of 87.99%. Next, the contribution of underlying surface changes to discharge changes is -3.71mm, accounting for 13.60% of the total. Meanwhile, the increase in potential evaporation contributes -0.44mm to discharge changes, with a contribution rate of -1.60%. Therefore, the primary cause of discharge changes is the increase in precipitation, followed by the impact of underlying surface changes. Specifically, the decrease in precipitation contributes to over 80% of discharge changes. This is mainly because the trend of potential evaporation from 2003 to 2020 is relatively small, while precipitation and discharge depth show a relatively large increasing trend. Consequently, evaporation and discharge depth are negatively correlated, while precipitation and discharge depth are positively correlated. Moreover, the positive contribution of precipitation to discharge depth exceeds the negative contribution of evaporation to discharge depth. Thus, the positive contribution to discharge increase mainly comes from precipitation, with a contribution rate exceeding 80%.

Table 3. Calculation results of hydrological elements to changes in basin discharge

Basin	contribution amount /mm			contribution percentage/%			discharge variation/mm	
	ΔR_P	ΔR_{E_0}	ΔR_{n}	C_P	C_{E_0}	C_n	ΔR_s	ΔR_m
Yellow River Inner Mongolia river	24.01	-0.44	3.71	87.99	-1.6	13.6	14.77	12.89

4.5. Discussion

Precipitation and changes in underlying surface are the two major factors leading to increased discharge, with the sensitivity of the underlying surface to discharge showing a growth trend, increasing by 22.3%. According to the research results of Sang(2021) on vegetation coverage in the Inner Mongolia region of the Yellow River Basin, the vegetation coverage in the Yellow River Basin has shown a gradually increasing trend. This has to some extent affected the changes in discharge, amplifying the impact of changes in the underlying surface on discharge.

Climate change and human activities are the two most important factors influencing changes in basin discharge. This study shows that the main factor affecting discharge changes in the Inner Mongolia section of the Yellow River Basin is precipitation variability, followed by changes in underlying surface. As seen in Figure 3, during the period from 2012 to 2020, precipitation was relatively abundant, with 6 years classified as above-normal or exceptionally wet years. In contrast, from 2003 to 2012, most years were below-normal or exceptionally dry, directly leading to an increase in basin discharge depth and further indicating that changes in precipitation conditions directly influence the trend of discharge variation.

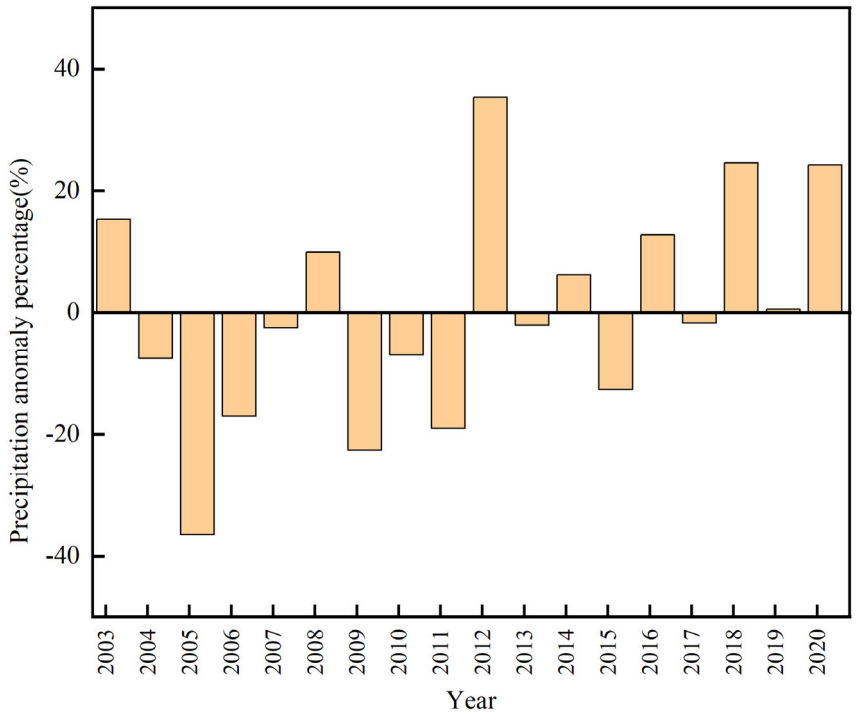

Figure 3. Percentage deviation of precipitation in the Yellow River Inner Mongolia Basin from 2003 to 2020.

5. CONCLUSIONS

(1)This study constructed a coupled hydrothermal model based on the water balance theory and Budyko hypothesis, and employed the GA algorithm to fit the model to obtain the optimal characteristic parameter \(n \). By using the parameters and hydrological data, the discharge changes at the head of the First Bend station in the Inner Mongolia section of the Yellow River were simulated. The Nash-Sutcliffe efficiency (NSE) of the simulated results compared to the measured data was 0.76, with a root mean square error (RMSE) of 10.45 mm and a relative root mean square error (RRMSE) of 19.5%, indicating a good consistency between the simulated and measured discharge depths.

(2)The discharge at the First Bend station shows a significant increasing trend, with a significant change point occurring in 2012. The interannual variation of precipitation is consistent with that of discharge, with peak and minimum values occurring at the same time, indicating the significant impact of precipitation on discharge changes. Sensitivity analysis of meteorological factors reveals that precipitation has the highest elasticity coefficient, indicating that discharge is more sensitive to changes in precipitation. This is followed by changes in underlying surface and potential evapotranspiration.

(3)The increase in precipitation contributes significantly to the changes in discharge in the Inner Mongolia section of the Yellow River basin, with a contribution rate as high as 88.79%. This is followed by changes in the underlying surface, with a contribution rate of 13.6%. The contribution rate of potential evaporation to discharge changes is relatively small. Therefore, it can be concluded that the significant increase in discharge after 2003 is mainly due to the increase in precipitation.

REFERENCES

[1] Zhang, J., et al. (2007). "Study on discharge trends of the six larger basins in China over the past 50 years. " Advances in Water Science 18(2): 230-234.

[2] Gan, G. J., et al. (2021). "Understanding interactions among climate, water, and vegetation with the Budyko framework." Earth-Science Reviews 212: 103451

[3] Gichamo, T., et al. (2023). "Ensemble rainfall-discharge modeling of physically based semi-distributed models using multi-source rainfall data fusion." Journal of Water and Climate Change. 15 (2): 325–347.

[4] Jia, K., et al. (2018). "Spectral matching based on discrete particle swarm optimization: A new method for terrestrial water body extraction using multi-temporal Landsat 8 images." Remote Sensing of Environment 209: 1-18.

[5] Jia, X. X., et al. (2020). "Regional Water Resources Assessment using Water Scarcity Pinch Analysis." Resources, Conservation and Recycling 157: 104749

[6] Miralles, D. G., et al. (2011). "Global land-surface evaporation estimated from satellite-based observations." Hydrol. Earth Syst. Sci. 15(2): 453-469.

[7] Ning, et al. (2016). "Separating the impacts of climate change and land surface alteration on discharge reduction in the Jing River catchment of China." Catena: An Interdisciplinary Journal of Soil Science Hydrology-Geomorphology Focusing on Geoecology and Landscape Evolution 147: 80-86.

[8] Ning, T., et al. (2017). "Vegetation dynamics and climate seasonality jointly control the interannual catchment water balance in the Loess Plateau under the Budyko framework." Hydrology and Earth System Sciences 21(3): 1515-1526.

[9] Rodell, M., et al. (2004). "The Global Land Data Assimilation System." Bulletin of the American Meteorological Society 85(3): 381-394.

[10] Yang, H., et al. (2008). "New analytical derivation of the mean annual water-energy balance equation." Water Resources Research 44(3):450

[11] Sang, J. (2021). "Climatic and Vegetation Ecological Changes in the Inner Mongolia Section of the Yellow River Basin from 1981 to 2017." Inner Mongolia Meteorology (01): 33-38+45.

[12] Shi, X., et al. (2020). "Prediction of Regional Water Resources Based on Variable Hydrothermal Coupling Balance Equation Parameters." Journal of North China University of Water Resources and Electric Power (Natural Science Edition) 41(01): 35-43.

[13] Song, W., et al. (2019). "Research Progress on Remote Sensing Monitoring of Surface Water Bodies." Satellite Applications(11): 41-47.

[14] Song, X., et al. (2005). "Analysis of Supply and Demand Contradictions Caused by Uneven Spatial Distribution of Water Resources in China." Arid Zone Research (02): 162-166.

[15] Yan, W., et al. (2023). "Attribution Analysis of Runoff Variation in Jinxi Basin Based on Budyko Hypothesis." Research of Soil and Water Conservation 30(03): 121-126.

[16] Yang, D., et al. (2015). "Attribution Analysis of Runoff Variation in Yellow River Basin Based on Water and Heat Coupling Balance Equation." Science in China: Technological Sciences 45(10): 1024-1034.

[17] Yang, H., (2021). "Temporal and Spatial Evolution Characteristics of Different River Types in the Inner Mongolia Section of the Yellow River and Their Causes Analysis." Inner Mongolia Agricultural University (D):23-27

[18] Yang, X., et al. (2023). "Attribution Identification of Runoff Changes in the Yihe River Basin Based on the Budyko Hypothesis." Research of Soil and Water Conservation 30(02): 100-106.

[19] Zhang, C., et al. (2022). "Research on the discharge Driving Mechanism in Zhenjiangguan Basin Based on the Coupled Hydrothermal Model." Water Resources and Hydropower Engineering 53(08): 78-87.

[20] Zhang, Q., et al. (2011). "Surface Water Resources Status in China from 1956 to 2000: Characteristics, Causes, and Impacts." Acta Geographica Sinica 31(12): 1430-1436.